

Chemicals

Nickel nitrate hexahydrate ($\text{Ni}(\text{NO}_3)_2 \cdot 6\text{H}_2\text{O}$, 98%), Ammonium molybdate ($(\text{NH}_4)_6\text{Mo}_7\text{O}_{24}$), 2-methylimidazole, Methanol, sulfuric acid (H_2SO_4), Nitric acid (HNO_3), ethanol ($\text{C}_2\text{H}_6\text{O}$), Deionized water, hydrogen peroxide (H_2O_2 , 30 wt%) were purchased from Lanyi Chemical Company (Beijing). The precursor of activated carbon was kindly provided by Beijing Jiahekailai Furniture and Design Company, which was obtained during the furniture manufacturing process containing 12% of ureaformaldehyde resin adhesive. All the chemicals were of analytical grade and used without further purification.

Preparation of AAC

The waste fiberboard, which was obtained in the furniture manufacturing process containing 10% ureaformaldehyde resin adhesive of the mass, was carbonized in a high-purity N_2 at the temperature increase rate of $10\text{ }^\circ\text{C}/\text{min}$ to the final temperature of $500\text{ }^\circ\text{C}$ and maintained for 2 h. Then the obtained products were activated that mixed with KOH at the mass ratio 3:1 at the temperature $750\text{ }^\circ\text{C}$ for 60 min in oven. After that, the prepared activated carbon was oxidized using the mixture of sulfuric and nitric acid as oxidization agent. Briefly, 3 g of activated carbon powder was mixed with 100 mL sulfuric and nitric acid solutions in round-bottom flask, and the solution was back flowed for 8 h under the temperature of $140\text{ }^\circ\text{C}$ in the oil bath. After natural cooling to room temperature, the solution was

centrifuged at 8000 rpm for 30 min to remove large amount of agglomerate particles. During the period, the distilled water was changed for several times to neutral.

Material characterization

The TecnaiTF20 Transmission electron microscopy (TEM, Netherlands) was used to investigate the morphologies and microstructure. Energy-dispersive spectroscopy (EDS) element analysis was also performed on the same instrument in TEM mode. X-ray diffraction (XRD) spectra were collected on D/max-2550 diffractometer with Cu $\kappa\alpha$ -1 radiation ($\lambda = 0.15406$ nm). The data of X-ray photoelectron spectroscopy (XPS) were recorded on Kratos Analytical Ltd by using Al $K\alpha$, $h\nu = 1486.7$ eV.

Electrochemical measurements

The electrochemical measurements of the fabricated A(B)-Ni_xMo_y-MOFs@AAC//activated carbon asymmetric supercapacitor were implemented in 7 M KOH aqueous electrolyte in a three-electrode cell at room temperature. The power density (P) and energy density (E) of the asymmetric supercapacitors were calculated according to the following equation:

$$C_m = (I\Delta t)/(M\Delta V) \quad [1]$$

$$E = (C_m\Delta V^2)/2 \quad [2]$$

$$P = E/\Delta t \quad [3]$$

Where C_m is the specific capacitance of A(B)-Ni_xMo_y-MOFs@AAC//activated carbon asymmetric supercapacitor (F g⁻¹) and M is the total mass of active materials on both electrodes, I is the discharge current (A), Δt is the discharge time (s), ΔV is the potential window during the discharge process except the ohmic drop (V). P is the power density and E is the energy density of the asymmetric supercapacitors.

Table S1. Composition of A(B)- Ni_xMo_y-MOFs@AAC hybrids

Samples	Activated carbon content (g)	Ni/Mo molar ratio	2-methylimidazole content (mmol)	Methanol content (ml)
A-Ni ₁ Mo _{0.2} -MOFs@AAC	0.1	1:0.2	3	100
A-Ni ₁ Mo _{0.4} -MOFs@AAC	0.1	1:0.4	3	100
A-Ni ₁ Mo _{0.5} -MOFs@AAC	0.1	1:0.5	3	100
A-Ni ₁ Mo _{0.6} -MOFs@AAC	0.1	1:0.6	3	100
B-Ni ₁ Mo _{0.2} -MOFs@AAC	0.1	1:0.2	3	100
B-Ni ₁ Mo _{0.4} -MOFs@AAC	0.1	1:0.4	3	100

MOFs@AAC

B-Ni₁Mo_{0.5}- 0.1 1:0.5 3 100

MOFs@AAC

B-Ni₁Mo_{0.6}- 0.1 1:0.6 3 100

MOFs@AAC

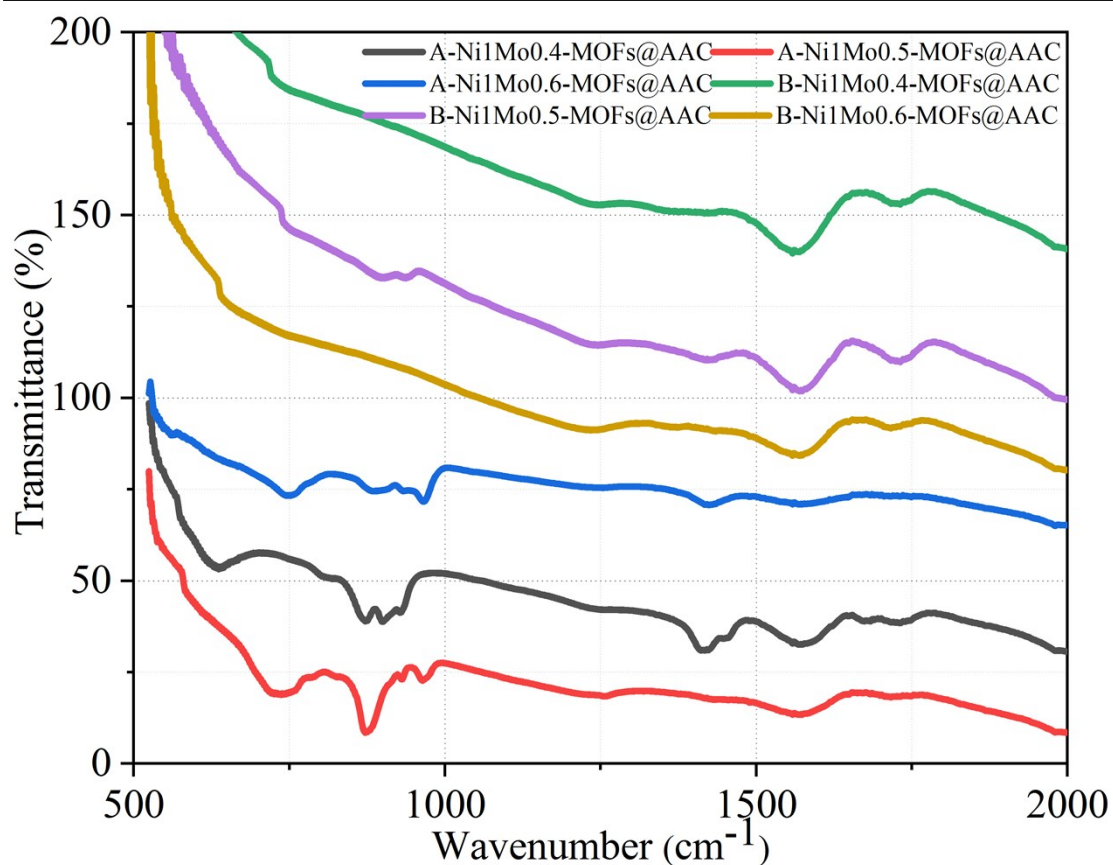


Fig.S1. The FT-IR spectra of A-Ni_xMo_y-MOFs@AAC hybrids

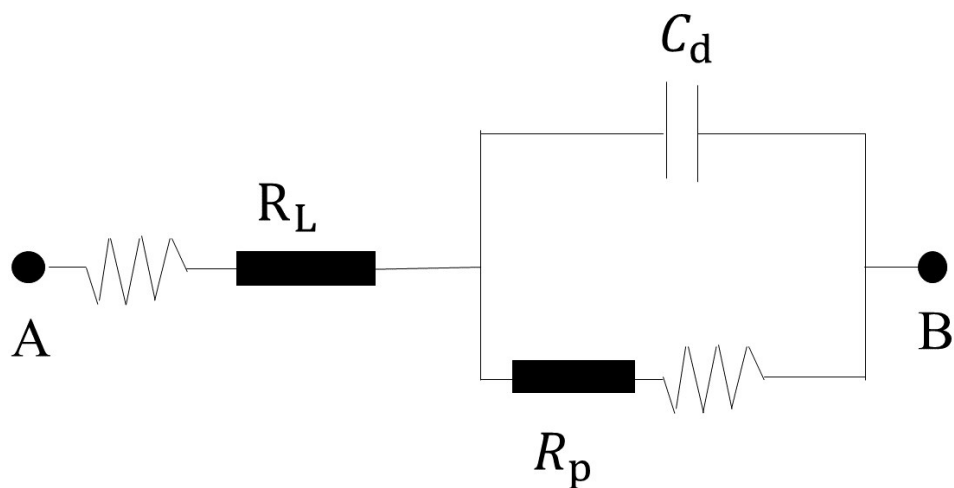


Fig.S2. The electrical equivalent circuit used for fitting impedance spectra.

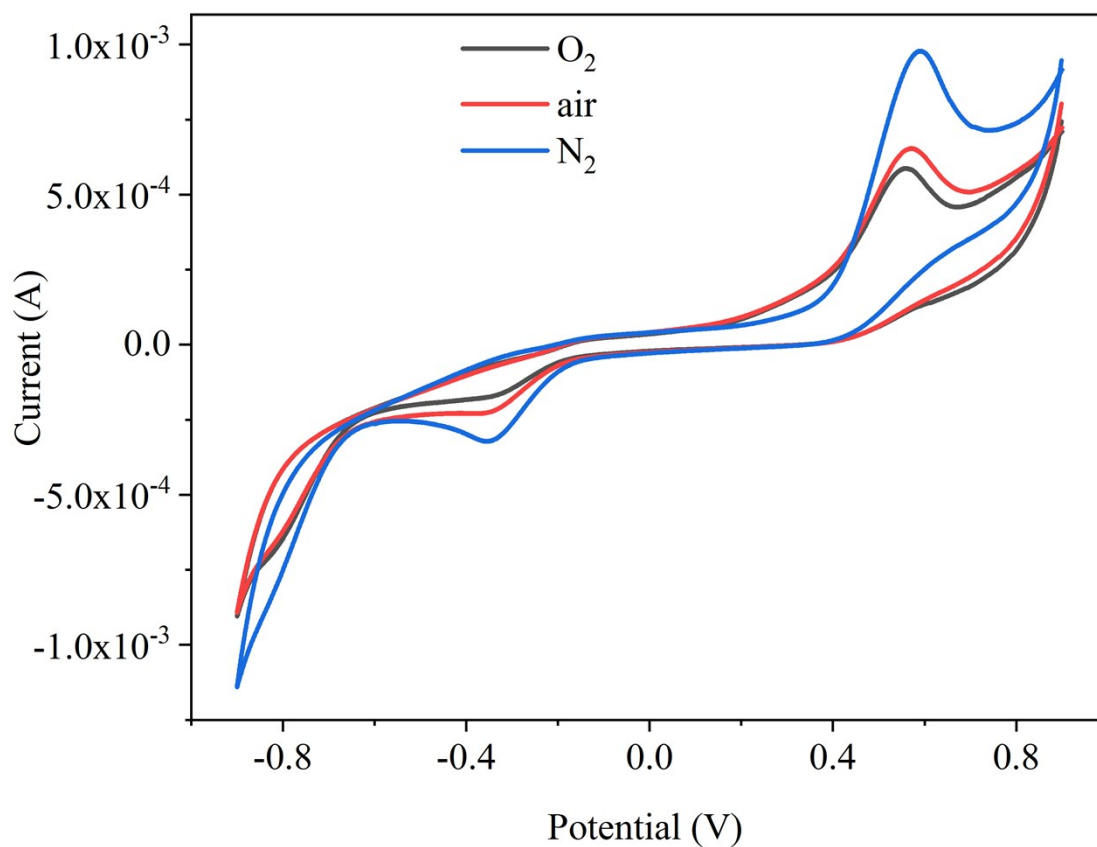


Fig.S3. cyclic voltammograms of A-Ni₁Mo_{0.5}-MOFs@AAC sensors by feeding with O₂, N₂ and air

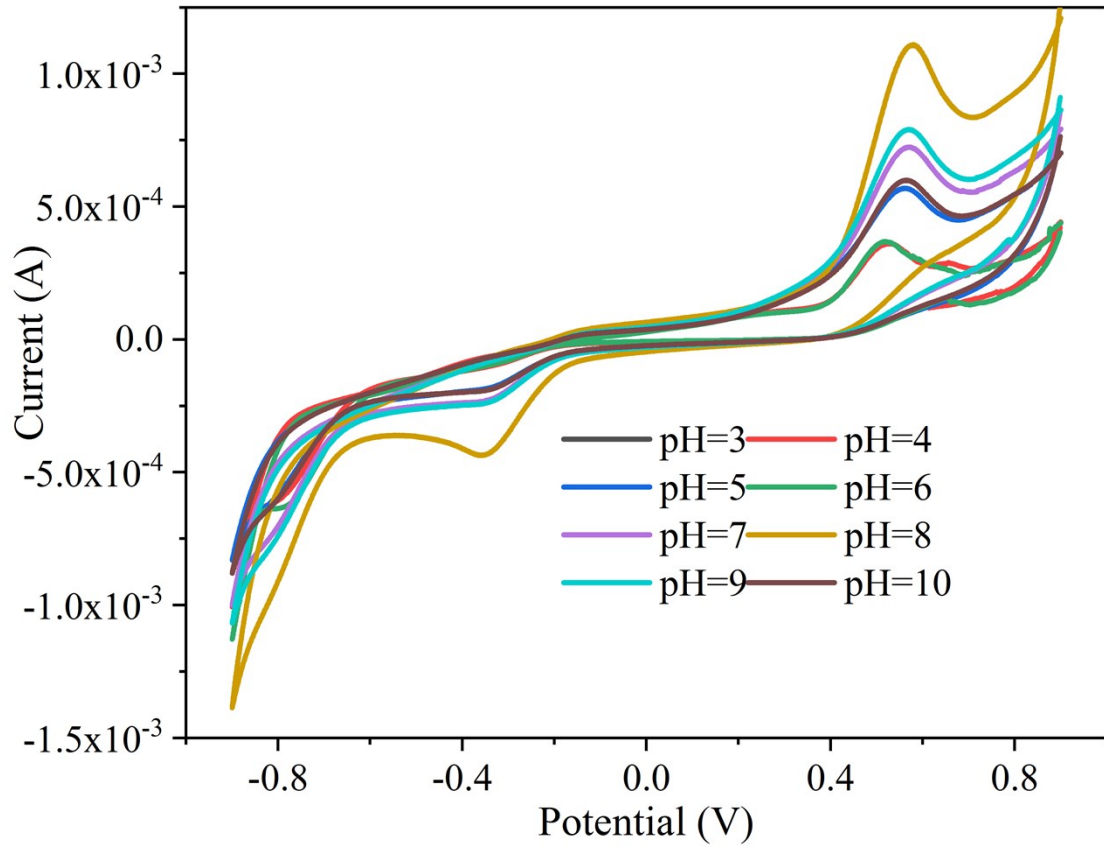


Fig.S4. cyclic voltammograms of A-Ni₁Mo_{0.5}-MOFs@AAC sensors in different pH solution

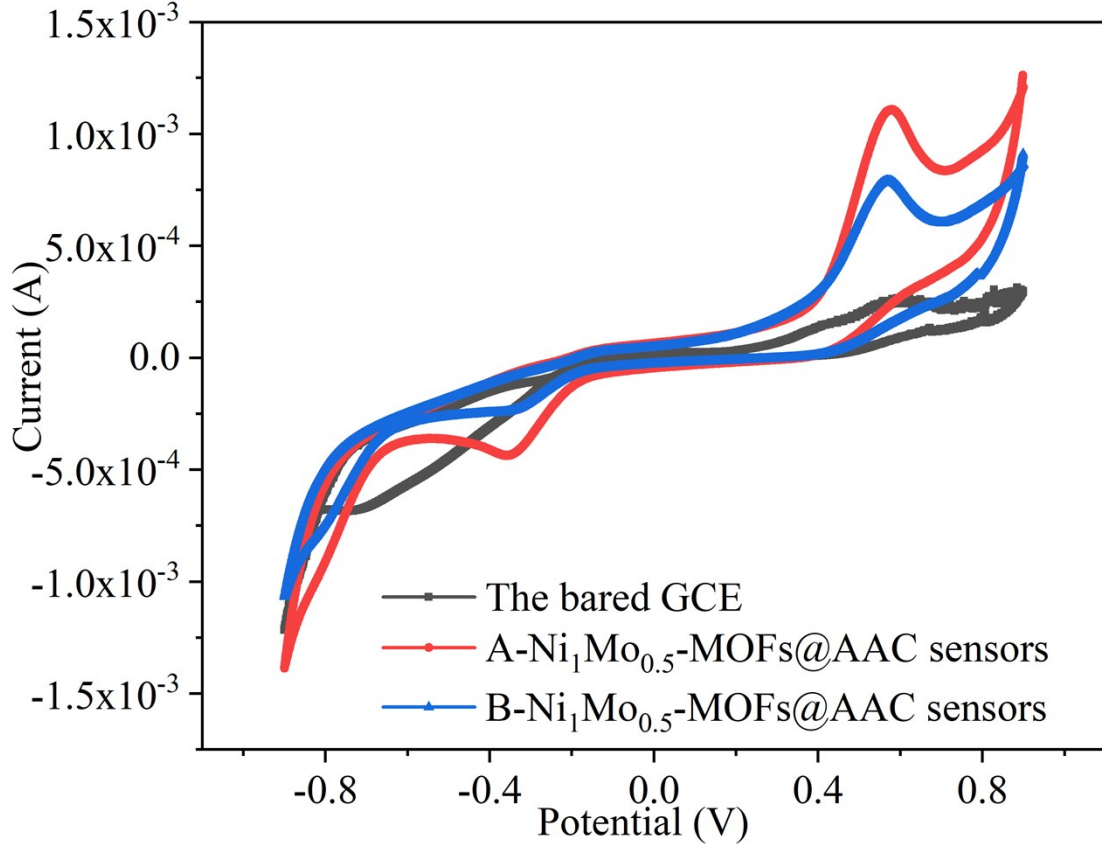


Fig.S5. cyclic voltammograms of bared GCE and A(B)-Ni₁Mo_{0.5}-MOFs@AAC sensors

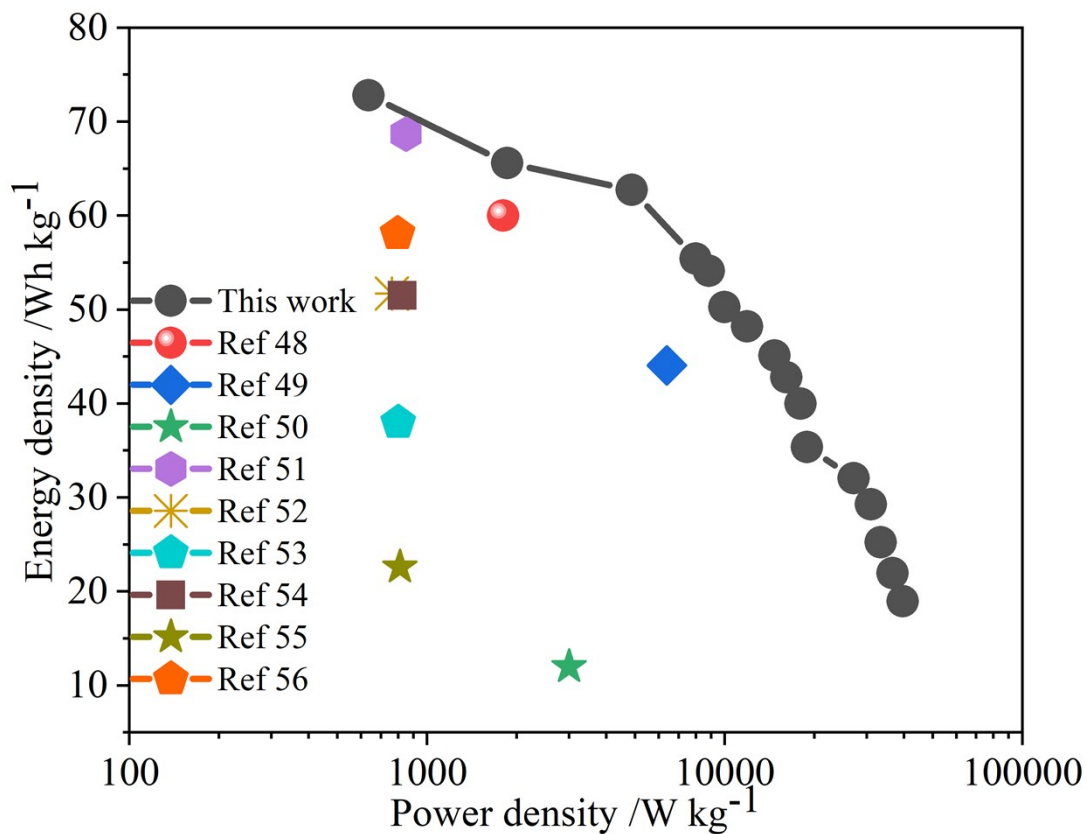


Fig.S6. The comparison of Ragone plot of our work and other Ref.

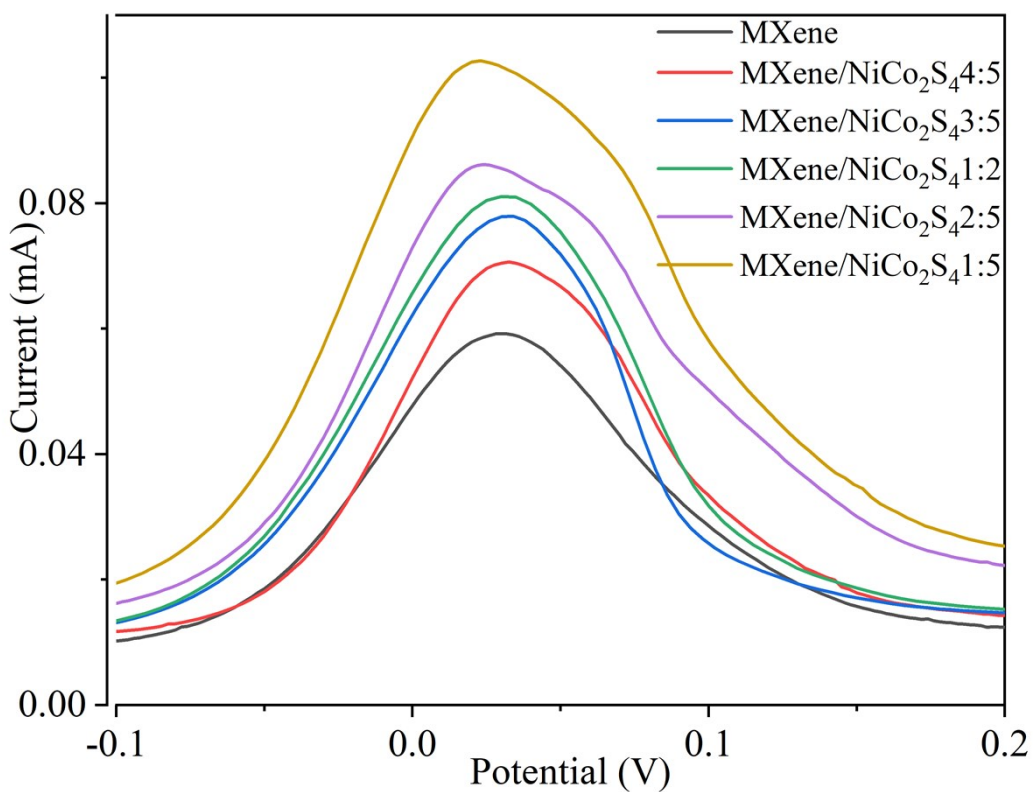


Fig.S7. DPV curves Of MXene and MXene/ NiCo_2S_4 hybrids for the concentration of H_2O_2 ($5 \mu\text{M}$)

Table S2. The properties of the various MOF of other hybrids modified electrodes for detection

Electrode	Electrolyte	Sensitivity		Detection	Linear	Ref
		$\mu\text{A } \mu\text{M}^{-1}$		limit	range	
				$\mu\text{M(S/N=3)}$	μM	
A-Pd _{0.2} Cd _{1.5} IF- 8@AAC	0.1 PBS (Ph=9.0)	0.266		0.016	2-1750	Ref.1
Co/Mn-MOFs	0.2 M NaAC (Ph=4.0)	---		0.85	1-100	Ref.2
Cr-MOFs	0.1 M NaOH	11.9		3.52	25-500	Ref.3
Poly caffeic acid@Zn/Ni-ZIF-8-800	PBS (pH=7.5)	---		0.0291	0.08-1000	Ref.4
Cu-TDPAT-n-GO/gce	PBS (pH=7.0)	---		0.17	4-12000	Ref.5
A-Ni ₁ Mo _{0.5} -MOFs	PBS (pH=8)	0.1985		0.18	2-1930	In this work

1. Y. Li, L. Xu, M. Jia, L. Cui, X. Liu and X. Jin, *Materials & Design*, 2020, **186**.
2. X. Qi, H. Tian, X. Dang, Y. Fan, Y. Zhang and H. Zhao, *Analytical Methods*, 2019, **11**, 1111-1124.
3. N. S. Lopa, M. M. Rahman, F. Ahmed, S. Chandra Sutradhar, T. Ryu and W. Kim, *Electrochimica Acta*, 2018, **274**, 49-56.
4. W. Zhang, L. Zong, S. Liu, S. Pei, Y. Zhang, X. Ding, B. Jiang and Y. Zhang, *Biosens Bioelectron*, 2019, **131**, 200-206.

5. C. Li, T. Zhang, J. Zhao, H. Liu, B. Zheng, Y. Gu, X. Yan, Y. Li, N. Lu, Z. Zhang and G. Feng, *ACS Appl Mater Interfaces*, 2017, **9**, 2984-2994.